Available online at www.sciencedirect.com
ScienceDirect
Journal of the European Ceramic Society 29 (2009) 2395–2402
www.elsevier.com/locate/jeurceramsoc

Reaction forming of silicon carbide ceramic using phenolic resin derived porous carbon preform

Shunjian Xu [a,*], Guanjun Qiao [a,*], Dichen Li [b], Hong Yang [c], Yinong Liu [c], Tianjian Lu [a]

[a] *State Key Laboratory for Mechanical Behavior of Materials, Xi'an Jiaotong University, Xi'an 710049, PR China*
[b] *School of Mechanical Engineering, Xi'an Jiaotong University, Xi'an 710049, PR China*
[c] *School of Mechanical Engineering, The University of Western Australia, Crawley, WA 6009, Australia*

Received 18 June 2008; received in revised form 9 January 2009; accepted 18 January 2009
Available online 17 March 2009

Abstract

SiC ceramics were prepared with porous carbon preforms derived from phenolic resin by a reaction-forming method. The effects of the structure of the preform pores and the infiltration process on the properties of SiC ceramics were investigated, and components with complex shapes were fabricated by combining this process with stereolithography (SLA). Dense SiC ceramics were obtained from carbon preforms with high apparent porosities, but SiC ceramics with many macrodefects resulted from a carbon preform with an apparent porosity of 39%. The infiltration of molten silicon into the preform pore channel was accelerated under vacuum pressure, resulting in an increase in the depth of the Si infiltration. The growth of SiC was predominantly controlled by carbon diffusion at the last stage of the reaction. The extended grain growth caused the SiC grains to coalesce and some free Si was enveloped in the SiC grains. SiC components with complex geometries were fabricated by combining reaction forming with SLA. The geometry was controlled by SLA.

Keywords: Sintering; Porosity; Microstructure; SiC; Engine components

1. Introduction

Silicon carbide (SiC) is a leading candidate for a wide variety of applications because of its superior mechanical properties at low and high temperatures, wear resistance, thermal properties and corrosion resistance.[1–11] Compared with other SiC forming processes, such as pressureless sintering, hot pressing and hot isostatic processing, reaction forming has two fundamental advantages[4–11]: (i) the ability to produce complex and near-net shapes and (ii) the ability to sinter at low temperatures and for short times. This process for producing SiC involves the preparation of a porous carbon preform and reactive infiltration of the preform with Si. The resulting SiC ceramic is known as reaction-formed SiC.

Porous carbon preform is usually fabricated through polymerization-induced phase separation and pyrolysis.[5–12] This liquid-based system for producing porous carbon preform was first described by Hucke.[6] In this approach, the carbon-yielding material is first mixed with a pore-forming agent. After curing, a rigid body is then obtained by polymerization-induced phase separation, which consists of two interconnected phases: a solid-state carbon-yielding material phase and a liquid-state pore-forming agent phase. The rigid body is then pyrolyzed to form a porous carbon preform while the pore-forming agent is removed. The morphology of the preform (e.g. pore size, apparent porosity and carbon wall thickness) can be controlled by changing the composition of the starting mixture. Furfuryl resin and furfural alcohol are often used as carbon-yielding materials.

During the reactive infiltration of the porous carbon preform, spontaneous wetting drives the Si melt to penetrate into the pore channels of the preform. The reaction between the Si melt and the carbon preform occurs at an elevated temperature during the infiltration process which forms the SiC.[13] The rate of infiltration and the reaction kinetics depend on the temperature and morphology of the preform. Many mechanisms have been proposed to describe the process of SiC growth including: the solution–precipitation mechanism,[14] a diffusion

* Corresponding authors. Fax: +86 29 82663453.
E-mail addresses: sjxu@yahoo.cn (S. Xu), gjqiao@mail.xjtu.edu.cn (G. Qiao).

0955-2219/$ – see front matter © 2009 Elsevier Ltd. All rights reserved.
doi:10.1016/j.jeurceramsoc.2009.01.022

mechanism[15–18] and an interface-limited mechanism.[19] However, the dominant mechanism is mostly dependent on the morphology of the preform. For porous carbon preforms with wall thicknesses less than 10 μm, the solution–precipitation mechanism has been proved to be the dominant mechanism for SiC growth.[20,21]

The desired shape of a SiC part is derived from the geometry of the preform, which is generally obtained by machining. However, the need for machining intrinsically limits the ability to produce complex shapes. An alternative method, which uses rapid prototyping (RP), can be applied to obtain the desired geometry of the preform.[22–24] Common RP techniques include: selective laser curing, selective laser sintering, stereolithography (SLA) and fused deposition modeling.

Phenolic resins have been increasingly used as precursors to produce various carbon materials, largely owing to their low cost and high carbon-yielding ratio.[25–27] In this study, porous carbon preforms derived from phenolic resin and prepared by means of polymerization-induced phase separation and pyrolysis, were used for the reaction-forming synthesis of SiC ceramics. The effects of the pore structure of the preform and the infiltration process on the morphologies and properties of the SiC ceramics were investigated. The complex-shaped components were fabricated by combining this process with SLA.

2. Experimental

2.1. Preparation of samples

Porous carbon preforms were prepared from a premix of three components: resol-type phenol–formaldehyde resin (industrial grade, viscosity: 0.975 Pa s), ethylene glycol (analytically pure, average molecular weight: 62.07) and benzenesulfonyl chloride (chemically pure, purity: 98.5%). Phenol–formaldehyde resin was employed as the carbon-yielding material, ethylene glycol as the solvent and pore-forming agent, and benzenesulfonyl chloride as the curing catalyst. These three materials were first stirred mechanically for 30 min at room temperature. The mixture was then poured into a glass tube and cured at a given temperature for 16 h. After curing, the cast was removed from the glass tube and then pyrolyzed by slowly heating to above 800 °C in a flowing N_2 atmosphere to produce a porous carbon preform. Preforms of differing pore structures were obtained by changing the compositions of the starting mixture and the polymerization conditions. The fabrication of porous carbon preforms has been described in detail elsewhere.[28]

Porous carbon preforms were machined into rectangular blocks of 12 mm × 10 mm × 50 mm, and then infiltrated with liquid Si at 1550 °C. The infiltration was conducted under two different atmospheric conditions: (i) nitrogen at 1 atm and (ii) vacuum atmosphere at 20 Pa. A BN-coated graphite crucible was needed for the liquid infiltration. Si powder (industrial grade, average particle size: 3–5 mm) was laid on the bottom of the crucible and the carbon preform was then placed on top of it. After the infiltration, the final product was cut and polished for microstructural observation.

A lost-mold method was applied to fabricate complex-shaped SiC parts. The lost mold was fabricated from a photo-curable resin by SLA. In this case, machining was not used and the excess Si on the sample surface was removed by vaporization at a high temperature.

2.2. Characterization

The morphologies of the porous carbon preforms and the synthesized SiC ceramics were characterized by means of optical microscopy, scanning electron microscopy (SEM) and energy dispersive spectroscopy (EDS) (JSM-7000F, Jeol, Japan). The pore size distributions, average pore size, bulk density and apparent porosity of the preforms were examined by a mercury porosimeter (PoreSizer 9320, Micromeritics, USA). The examined pore size distribution covered the range from 300 μm to 9 nm. All the samples were degassed under vacuum at 300 °C for 120 min before being measured.

The density of the synthesized SiC ceramics was determined by Archimedes' method. Their excess free Si was removed by chemical etching for 24 h in a 70 wt.%HF–30 wt.%HNO_3 solution at room temperature. The volume fraction of the free Si was calculated by weighing the samples before and after the etching. The volume fraction of unreacted carbon in the SiC product was determined by image analysis. X-ray diffraction (XRD) measurements (D/max2400, Rigaku, Japan) were carried out on the powdered SiC ceramics using filtered Cu Kα radiation. The three-point flexural strength of the SiC ceramics was measured by an Instron 1195 universal testing machine (using 3 mm × 4 mm × 30 mm samples) using a loading rate of 0.5 mm min^{-1}. Five specimens were tested for each sample condition.

The weight loss behaviors of the phenolic resin and photo-curable resin were analyzed by a thermogravimetric analyser (TGA2950, TG, USA). The measurements were conducted by heating to 800 °C at a heating rate of 10 °C/min in flowing N_2.

3. Results and discussion

3.1. Preparation of preforms

Fig. 1 shows the effect of the concentration of the curing catalyst on the apparent porosity of preforms cured at 100, 140 and 180 °C. It indicates that the apparent porosity of the preform increases with the increasing concentration of the catalyst and as the curing temperature rises. The apparent porosity can be controlled within the range 23–54%.

Singh and Behrendt[11] have reported that carbon preform cannot be completely infiltrated with liquid Si when the porosity of the carbon preform is below a critical value of 38%. This phenomenon is known as choking-off. Thus, three preforms with apparent porosities of 45.5, 45.1 and 38.9%, designated respectively, as PC-A, PC-B, and PC-C were selected to conduct Si infiltration. SEM micrographs of the selected porous carbon preforms are shown in Fig. 2. It can be clearly seen that all three preforms consist of uniformly distributed and intercon-

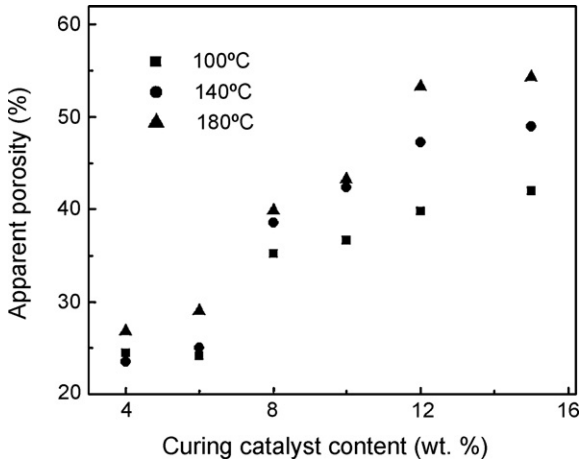

Fig. 1. Effect of curing catalyst concentration on apparent porosity of porous carbon preforms prepared at curing temperatures of 100, 140 and 180 °C.

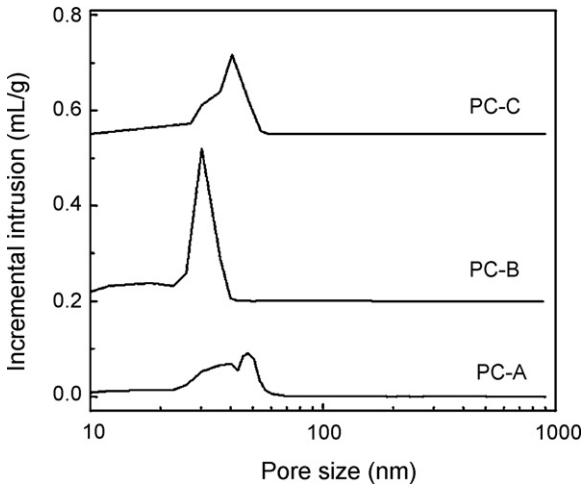

Fig. 3. Pore size distributions of porous carbon preforms.

nected pores and carbon skeletons. PC-B appears to have smaller pore sizes and thinner carbon walls than PC-A and PC-C. Fig. 3 shows the pore size distributions of the three preforms. It is obvious that they all have very narrow pore size distributions. The physical properties of the three preforms are summarized in Table 1, which shows that the average pore size varies in the range 29–40 nm, PC-B being the smallest. The apparent porosities of PC-B and PC-C differ considerably and the values of their bulk densities are very close. Similarly, PC-A and PC-B are very close in apparent porosities but differ in bulk densities.

3.2. Reactive infiltration of preforms under vacuum pressure

All three preforms are completely infiltrated with liquid Si at 20 Pa infiltration pressure. The corresponding SiC ceramics were labelled as SC-A, SC-B and SC-C, respectively. The microstructures of the SiC samples are shown in Figs. 4–6 and the properties of the samples are listed in Table 2.

Fig. 4 shows the microstructures of SC-A10 and SC-A30 prepared from PC-A preform at 1550 °C for 10 and 30 min, respectively. Images (a) and (b) are optical micrographs. These samples are composed of polygonal SiC grains (the gray phase)

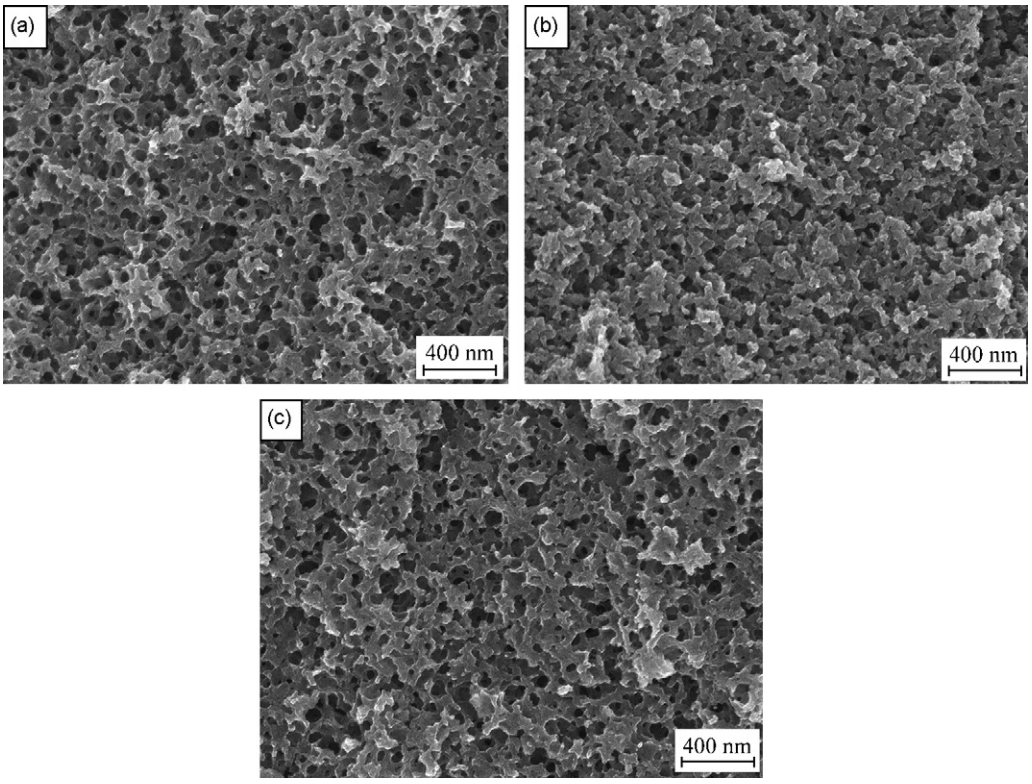

Fig. 2. SEM micrographs of porous carbon preforms: (a) PC-A, (b) PC-B and (c) PC-C.

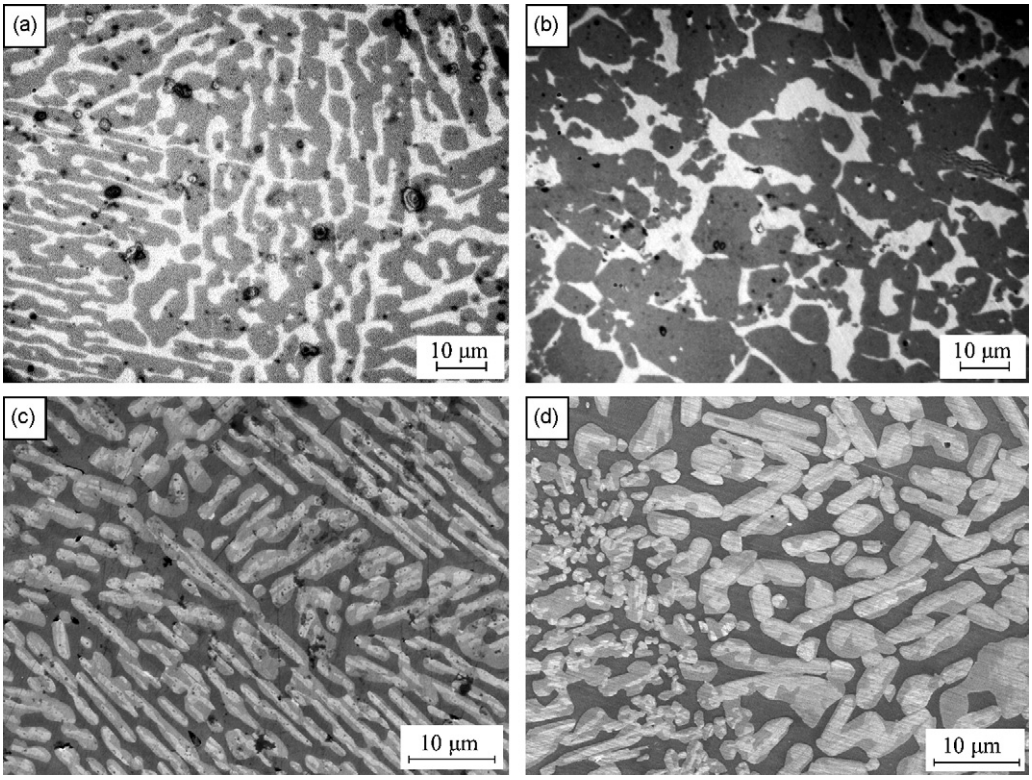

Fig. 4. Optical micrographs (a and b) and secondary electron SEM images (c and d) of SiC ceramics: (a) and (c) SC-A10, (b) and (d) SC-A30.

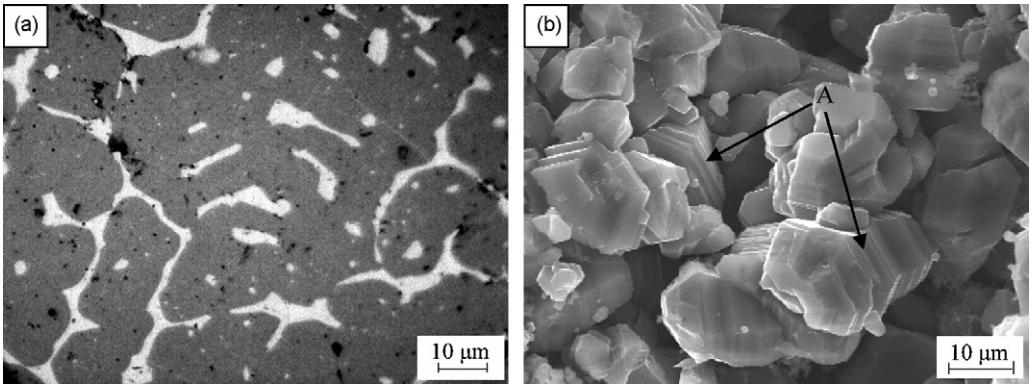

Fig. 5. Micrographs of SC-B: (a) optical micrograph, (b) SEM image of SiC grains. Serrated growth fronts of SiC grains in (b) indicate epitaxial growth of SiC.

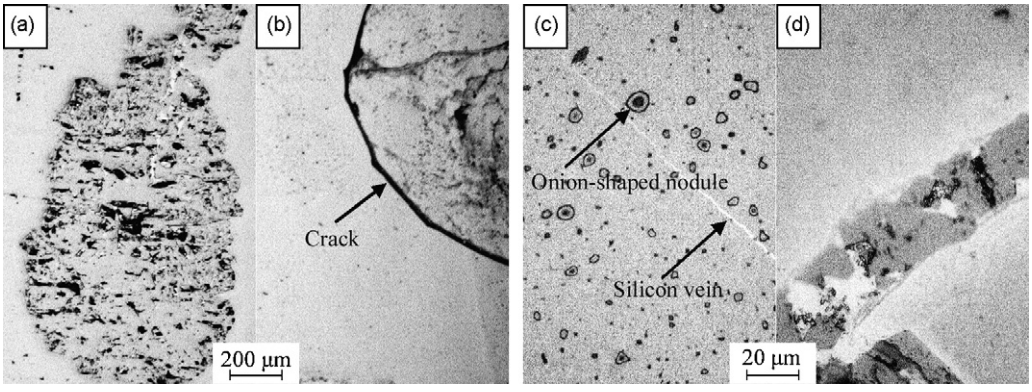

Fig. 6. Optical micrographs of SC-C showing five kinds of macrodefect: (a) unordered nodules, (b) crack, (c) onion-shaped nodules and silicon vein, (d) vein filled with coarse SiC.

Table 1
Physical properties of porous carbon performs.

Sample	Apparent porosity (%)	Average pore size (nm)	Bulk density (g cm^{-3})
PC-A	45.5 ± 0.3	39.9 ± 0.3	0.72
PC-B	45.1 ± 0.3	28.8 ± 0.2	0.79
PC-C	38.9 ± 0.4	38.7 ± 0.3	0.78

infiltrated with a continuous network of free Si (the white phase). Compared with the SiC grains in SC-A10 which are elongated to 5–10 μm in length and are more uniformly distributed, those in SC-A30 appear to be more irregular and their grain size has an obvious bimodal distribution, with both large (up to 10 μm) and small (about 1 μm) grains. A small amount of unreacted carbon (the black phase) is also observed in the two samples. It is embedded in SiC grains and the volume fraction decreases from 4.2 to 0.3% when the infiltration time extends from 10 to 30 min, as shown in Table 2. Micrographs (c) and (d) are secondary electron SEM images of the two samples. There is a considerable contrast within the SiC grains, indicating compositional variations. The contrast is believed to be due to the nonuniform distribution of trace amounts of impurities within the grains.[29] The impurities come from the Si powder which has been used. It has been observed that the precipitation of SiC from Si melts is accompanied by the rejection of impurities to the liquid.[30] Thus, the first SiC formed at the core is purer and appears paler than the SiC formed later in the outer shell of the Si grains.

The flexural strength of SC-A30 is more than twice that of SC-A10 (see Table 2). At the same time, both the volume fraction of free Si and the residual carbon of SC-A10 are higher than that of SC-A30, implying that less in situ reaction is needed to form SiC for the SC-A10, obviously due to insufficient reaction time. This is believed to be the reason for the lower flexural strength of the SC-A10.

Fig. 5 shows the microstructure of SC-B prepared from PC-B at 1550 °C for 30 min. The optical micrograph shown in (a) reveals that SC-B has a similar microstructure to that of SC-A30. The volume fraction of free Si is lower and that of unreacted carbon is higher than that of SC-A30. The volume fraction of unreacted carbon in SC-B is 1.8% and that of free Si is 12.2%. The flexural strength of SC-B is lower than that of SC-A30. Less free Si in SC-B is due to the higher bulk density of the preform which was used, and the lower flexural strength may be caused by the increased amount of unreacted carbon in the sample. Fig. 5b is a SEM image of the sample (after etching for 24 h in a 70 wt.%HF–30 wt.%HNO_3 solution at room temperature). It reveals serrated growth fronts on the surface of the SiC grains, as indicated by the arrows, implying that the SiC grains grow by a liquid epitaxial growth mechanism.[17]

Based on the evidence presented in Figs. 4 and 5, it can be concluded that the growth of SiC is predominantly controlled by the diffusion of carbon in SiC at the final stage of the reaction, since both the grain boundary diffusion and the lattice diffusion coefficients of carbon in SiC are considerably higher than the lattice diffusion coefficient of Si. The unreacted carbon embedded in the SiC grains diffuses through the SiC layer and dissolves in the Si melt, then deposits onto the SiC which has already formed, thus resulting in the growth of the SiC grains. The extended growth causes the SiC grains to coalesce and Si is enveloped in them.

Fig. 6 shows the microstructure of SC-C prepared from PC-C at 1550 °C for 30 min. The sample has many surface cracks and defects. Five kinds of macrodefects can be identified: disordered nodules of unreacted carbon imbedded in SiC (Fig. 6a), cracks (Fig. 6b), Si veins (Fig. 6c), onion-shaped nodules of unreacted carbon (Fig. 6c) and veins filled with coarse SiC grains (Fig. 6d). The onion-shaped carbon nodules were also observed in SC-A10 (Fig. 4a). These macrodefects in SC-C led to a lower density and poor mechanical properties.

Disordered nodules, cracks and Si veins have commonly been observed in reaction-formed and reaction-bonded SiC.[5,11,17,31] These macrodefects occur as a result of using unsuitable preforms and imperfect technical conditions. Ness and Page[17] have suggested that disordered nodules are caused by heterogeneous pores in the preform, which may be eliminated by good compact mixing. Si veins and cracks occur as a result of thermal stresses generated during reaction or upon cooling. The short time and extreme temperature transients inherent in reactive infiltration may easily induce internal stresses. In this work, the occurrence of these macrodefects in SC-C may be due to insufficient pore volume in the preform, considering the relatively uniform pores in PC-C as well as the inexistence of Si veins and cracks in SC-A30 prepared from a preform of higher apparent porosity.

SiC is a covalentally bonded compound with several crystalline structures, of which α-SiC and β-SiC are the most common types. β-SiC changes slowly to the α-SiC format above 2100 °C. It has been reported that the exothermic reaction of Si + C may increase the local temperature to 500 °C and some newly formed β-SiC may change to α-SiC.[21] Fig. 7 shows the XRD spectra of SC-A10, SC-A30 and SC-B. Here, α-SiC is found in SC-B but not in SC-A10 and SC-A30. This suggests that the reactive infiltration of PC-B, which has smaller pores, induces a higher localized temperature.

Table 2
Properties of SiC ceramic samples.

Sample	Porous carbon preform	Time (min)	Silicon content (vol.%)	Unreacted carbon content (vol.%)	Density (g cm^{-3})	Flexural strength (MPa)
SC-A10	PC-	10	20	4.2	2.92	204 ± 55
SC-A30	A	30	15.4	0.3	3.07	445 ± 35
SC-B	PC-B	30	12.2	1.8	3.08	239 ± 41
SC-C	PC-C	30	3.1	7.1	2.95	60 ± 36

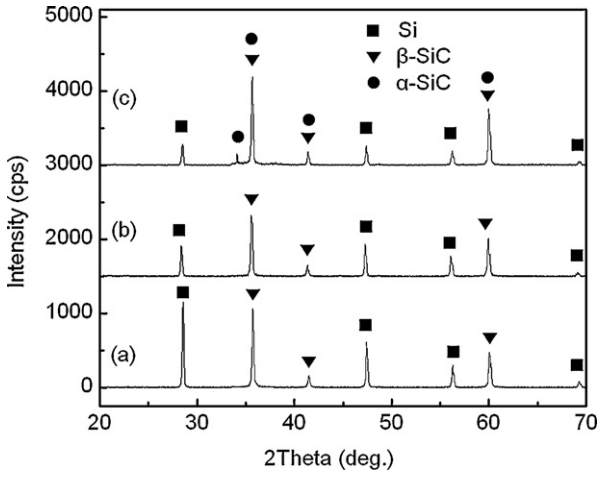

Fig. 7. XRD patterns of SiC ceramic: (a) SC-A10, (b) SC-A30, and (c) SC-B.

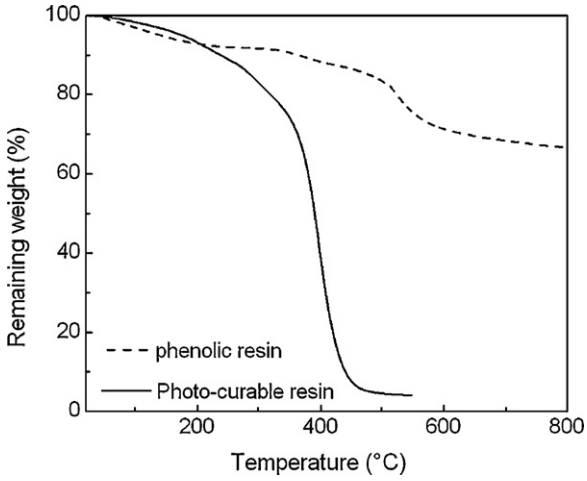

Fig. 9. TG curves for photo-curable resin and phenolic resin.

3.3. Reactive infiltration of preforms at ambient pressure

The three porous carbon preforms were not completely infiltrated with liquid Si when they were infiltrated at 1 atm pressure N_2. In other words, the choking-off of the infiltration occurred. Under this condition, the entire surface of the preform may be uniformly coated even though only one side of the preform is in contact with the liquid Si. Fig. 8 shows SEM micrographs of the cross-sections and an elemental concentration profile of a partially infiltrated sample prepared from PC-A. Three layers can be clearly identified at the microscopic level, as shown in Fig. 8a: an unreacted carbon layer, a transition layer and a reacted layer. The transition layer contains some pores mixed with SiC grains and Si, as shown in Fig. 8b. These pores are formed by the stacking of newly formed SiC grains. The reacted layer is dense and consists of SiC grains and Si, as shown in Fig. 8c.

When a porous carbon preform is infiltrated at 1 atm, spontaneous wetting is the only driving force, which causes the Si melt to penetrate into the pore channels of the preform. At the same time, the reaction between Si and C occurs to form SiC. Using the Poiseuille capillary flow equation, the time, t, to attain an infiltration depth x is given by[32]

$$t = x^2 \left[\frac{\gamma r (r^3/r_0^2 R)\cos\ \Theta}{2\eta} \right]^{-1} \quad (1)$$

where γ is the surface tension of liquid Si, η is the viscosity of liquid Si, Θ is the contact angle, R is the effective capillary radius, r_0 is the mean geometrical capillary radius, and r is the effective fluid radius ($r < R < r_0$). In view of the microstructure of the SiC ceramics, the growth of SiC grains is controlled by a solution–precipitation mechanism at the early and intermediate stages of the reaction. Thus, the degree of advancement of the reaction is followed by determinations of the volume fraction of carbon after successive periods of infiltration.[14] The time required for the dissolution of the carbon in molten Si can be estimated as[14]

$$\Delta y = \frac{\sqrt{(D)} c_e}{2\rho_c} \sqrt{(t)} \quad (2)$$

where Δy is the thickness of the dissolved layer of C after time t, ρ_c is the density of the carbonaceous material which dissolves, c_e is the equilibrium solubility of carbon in liquid Si, and D is the diffusion coefficient of carbon in liquid Si. Substituting literature data[14,33] into Eqs. (1) and (2), the full infiltration of

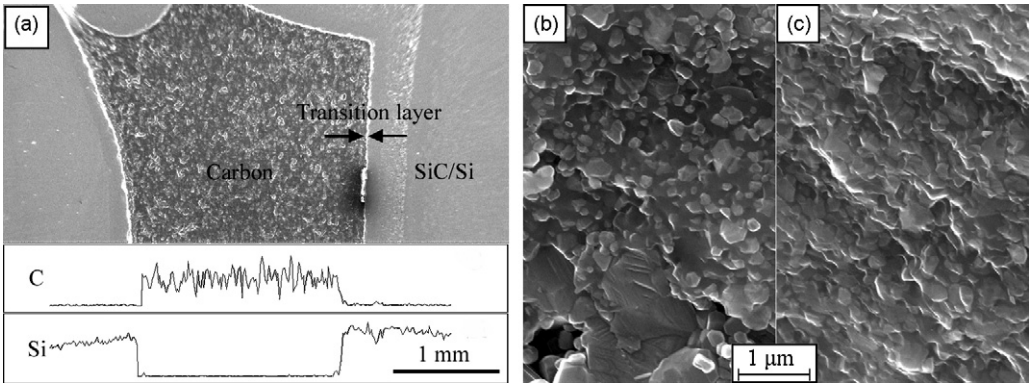

Fig. 8. SEM micrographs of partial infiltration sample: (a) elemental concentrations of the cross-section, (b) transition layer, and (c) reacted layer.

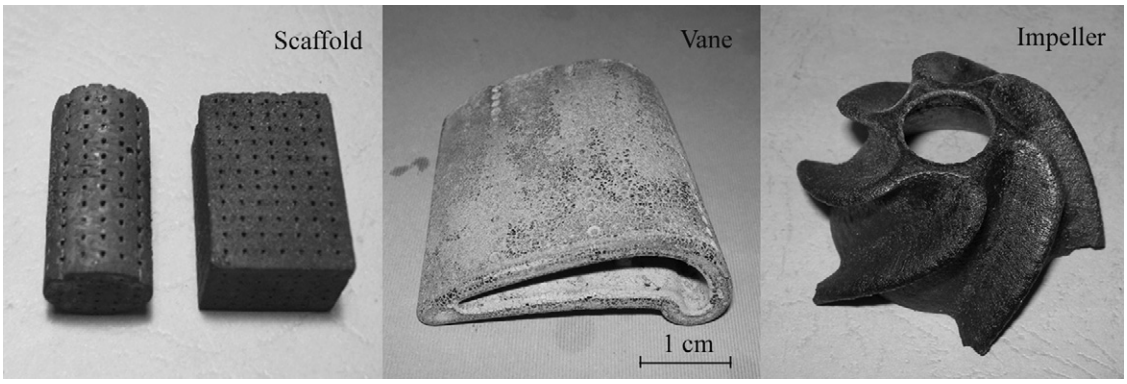

Fig. 10. SiC parts fabricated by combining reaction forming with SLA. Scale bar is the same for all three images.

10 mm preform thickness requires $t = 20$–2 s for $r = 10$–100 nm (assuming $r = R = r_0$), and a carbon wall thickness of 100 nm is dissolved in about 1 s. It is obvious that the infiltration rate is slower than the reaction rate. The newly formed SiC acts as a reaction barrier to further rapid infiltration of liquid Si, resulting in choking-off of the infiltration in preforms with dimensions of 1 cm. In contrast, when a porous carbon preform was infiltrated at 20 Pa, the infiltration of molten Si into the preform pore channel was accelerated under vacuum pressure, resulting in full infiltration in preforms with the same dimensions.

3.4. Evaluation of complex shapes

Fig. 9 reveals the weight loss of the photo-curable resin and phenolic resin. It should be noted that the remaining weight of the photo-curable resin is below 5% after heating to 500 °C whereas the remaining weight of the phenolic resin is ~66% at 800 °C. This result indicates that the lost mold can be almost completely removed at a pyrolysis temperature of 800 °C. The weight losses of the phenolic resin and photo-curable resin are associated with the release of volatiles of unimolecules, such as H_2O, CO, CO_2, H_2 and other gases.[34]

Fig. 10 shows some SiC parts prepared by combining reaction forming with SLA. The volume shrinkage of the SiC parts is about 8% and there is no distortion.

4. Conclusions

Porous carbon preforms derived from phenolic resin have been prepared by polymerization-induced phase separation and pyrolysis. The properties of these preforms can be controlled by controlling the composition of the pre-mixture and the polymerizing conditions. Three preforms with apparent porosities from 38.9 to 45.5% were selected to fabricate SiC ceramics by reaction forming. The dense SiC ceramic, which was typically composed of polygonal SiC grains and a small fraction of free Si was obtained from carbon preforms with high apparent porosities. The volume fraction of free Si, flexural strength and density were 15.4%, 445 ± 35 MPa and 3.07 g cm^{-3}, respectively. It has also been shown that the infiltration of molten Si into the pore channels of the preform was accelerated under vacuum pressure, resulting in an increase in the depth of the Si infiltration. The growth of SiC was predominantly controlled by carbon diffusion through SiC at the final stage of the reaction. The extended grain growth caused coalescence of SiC grains and the envelopment of some free Si in the SiC grains.

Complex-shaped SiC parts have been prepared by combining reaction forming with SLA, and the geometry of SiC parts was controlled by SLA. The volume shrinkage of the SiC parts was about 8% and no distortion occurred.

Acknowledgements

This work was supported by the National Natural Science Foundation of China (NSFC, 50475082 and 50835007), the National Basic Research Program of China (973, 2006CB601200) and the Gledden Senior Visiting Fellowship of The University of Western Australia.

References

1. Jin, H. Y., Ishiyama, M., Qiao, G. J., Gao, J. Q. and Jin, Z. H., Plasma active sintering of silicon carbide. *Mater. Sci. Eng. A*, 2008, **483/484**, 270–273.
2. van Veggel, A. A., van den Ende, D., Bogenstahl, J., Rowan, S., Cunningham, W., Gubbels, G. H. M. *et al.*, Hydroxide catalysis bonding of silicon carbide. *J. Eur. Ceram. Soc.*, 2008, **28**, 303–310.
3. Yoon, T. H., Lee, H. J., Yan, J. and Kim, D. P., Fabrication of SiC-based ceramic microstructures from preceramic polymers with sacrificial templates and lithographic techniques—a review. *J. Ceram. Soc. Jpn.*, 2006, **114**, 473–779.
4. Cui, Z. Z., Li, D. C., Qiao, G. J., Lei, X. and Hou, H., Preparation of complex-shape SiC ceramic composites parts derived from phenolic resin template. *Acta Mater. Comp. Sin.*, 2006, **23**, 138–143.
5. Wang, Y. X., Tan, S. H. and Jiang, D. L., The effect of porous carbon preform and the infiltration process on the properties of reaction-formed SiC. *Carbon*, 2004, **42**, 1833–1839.
6. Hucke, E. E., Methods of producing carbonaceous bodies and the products thereof. US patent 3,859,421; 1975.
7. Chiang, Y. M., Messner, R. P., Terwilliger, C. D. and Behrendt, D. R., Reaction-formed silicon carbide. *Mater. Sci. Eng. A*, 1991, **144**, 63–74.
8. Hozer, L., Lee, J. R. and Chiang, Y. M., Reaction-infiltrated, net-shape SiC composites. *Mater. Sci. Eng. A*, 1995, **195**, 131–143.
9. Fernández, J. M., Muñoz, A., López, A. R. D., Feria, F. M. D., DomÍnguez-RodrÍguez, A. and Singh, M., Microstructure-mechanical properties correlation in siliconized silicon carbide ceramics. *Acta Mater.*, 2003, **51**, 3259–3275.
10. Fernández, J. M., Muñoz, A., Varela-Feria, F. M. and Singh, M., Interfacial and thermomechanical characterization of reaction formed joints in silicon carbide-based materials. *J. Eur. Ceram. Soc.*, 2000, **20**, 2641–2648.

11. Singh, M. and Behrendt, D. R., Reactive melt infiltration of silicon-molybdenum alloys into microporous carbon preforms. *Mater. Sci. Eng. A*, 1995, **194**, 193–200.
12. Wang, Y. X., Tan, S. H., Jiang, D. L. and Zhang, X. Y., Preparation of porous carbon derived from mixtures of furfuryl resin and glycol with controlled pore size distribution. *Carbon*, 2003, **41**, 2065–2072.
13. Cai, N., Ma, R., Qiao, G. J. and Jin, Z. H., Reaction mechanism of silicon carbide ceramics derived from woods. *J. Inorg. Mater.*, 2001, **16**, 763–768.
14. Pampuch, R., Walasek, E. and Bialoskorski, J., Reaction-mechanism in carbon liquid silicon systems at elevated-temperatures. *Ceram. Int.*, 1986, **12**, 99–106.
15. Fitzer, E. and Gadow, R., Fiber-reinforced silicon-carbide. *Am. Ceram. Soc. Bull.*, 1986, **65**, 326–335.
16. Li, J. G. and Hausner, H., Reactive wetting in the liquid-silicon/solid-carbon system. *J. Am. Ceram. Soc.*, 1996, **79**, 873–880.
17. Ness, J. N. and Page, T. F., Microstructural evolution in reaction-bonded silicon carbide. *J. Mater. Sci.*, 1986, **21**, 1377–1397.
18. Zhou, H. and Singh, R. N., Kinetics model for the growth of silicon carbide by the reaction of liquid silicon with carbon. *J. Am. Ceram. Soc.*, 1995, **78**, 2456–2462.
19. Hase, T., Suzuki, H. and Iseki, T., Formation process of β-SiC during reaction-sintering. *J. Nucl. Mater.*, 1976, **59**, 42–48.
20. Zollfrank, C. and Sieber, H., Microstructure evolution and reaction mechanism of biomorphous SiSiC ceramics. *J. Am. Ceram. Soc.*, 2005, **88**, 51–58.
21. Varela-Feria, F. M., Ramírez-Rico, J., de Arellano-López, A. R., Martínez-Fernández, J. and Singh, M., Reaction-formation mechanisms and microstructure evolution of biomorphic SiC. *J. Mater. Sci.*, 2008, **43**, 933–941.
22. Friedel, T., Travitzky, N., Niebling, F., Scheffler, M. and Greil, P., Fabrication of polymer derived ceramic parts by selective laser curing. *J. Eur. Ceram. Soc.*, 2005, **25**, 193–197.
23. Guo, D., Li, L. T., Cai, K., Gui, Z. L. and Nan, C. W., Rapid prototyping of piezoelectric ceramics via selective laser sintering and gelcasting. *J. Am. Ceram. Soc.*, 2004, **87**, 17–22.
24. Taboas, J. M., Maddox, R. D., Krebsbacha, P. H. and Hollister, S. J., Indirect solid free form fabrication of local and global porous, biomimetic and composite 3D polymer-ceramic scaffolds. *Biomaterials*, 2003, **24**, 181–194.
25. Wei, W., Qin, G. T., Hu, H. Q., You, L. B. and Chen, G. H., Preparation of carbon molecular sieve membrane from phenol–formaldehyde novolac resin. *Carbon*, 2002, **40**, 465–467.
26. Ozaki, J., Endo, N., Ohizumi, W., Igarashi, K., Nakahara, M., Oya, A. *et al.*, Novel preparation method for the production of mesoporous carbon fiber from a polymer blend. *Carbon*, 1997, **35**, 1031–1033.
27. Kosonen, H., Valkama, S., Nykänen, A., Toivanen, M., ten Brinke, G., Ruokolainen, J. *et al.*, Functional porous structures based on the pyrolysis of cured templates of block copolymer and phenolic resin. *Adv. Mater.*, 2006, **18**, 201–205.
28. Xu, S. J., Qiao, G. J., Wang, H. J., Li, D. C. and Lu, T. J., Preparation of mesoporous carbon derived from mixtures of phenol–formaldehyde resin and ethylene glycol. *Mater. Lett.*, 2008, **62**, 3716–3718.
29. Sawyer, G. R. and Page, T. F., Microstructural characterization of REFEL (reaction-bonded) silicon carbides. *J. Mater. Sci.*, 1978, **13**, 885–904.
30. Bechmann, G. E. J., The growth of silicon carbide from molten silicon. *J. Electrochem. Soc.*, 1963, **110**, 84–86.
31. Messner, R. P. and Chiang, Y. M., Liquid-phase reaction-bonding of silicon carbide using alloyed silicon-molybdenum melts. *J. Am. Ceram. Soc.*, 1990, **73**, 1193–1200.
32. Hillig, W. B., Melt infiltration approach on ceramic matrix composites. *J. Am. Ceram. Soc.*, 1988, **71**, C96–C99.
33. Greil, P., Lifka, T. and Kaindl, A., Biomorphic cellular silicon carbide ceramics from wood. I. Processing and microstructure. *J. Eur. Ceram. Soc.*, 1998, **18**, 1961–1973.
34. Trick, K. A. and Saliba, T. E., Mechanisms of the pyrolysis of phenolic resin in a carbon/phenolic composite. *Carbon*, 1995, **33**, 1509–1515.